Journal of Applied Polymer Science

Biocomposites based on poly(lactic acid) and seaweed wastes from agar extraction: Evaluation of physicochemical properties

Tomás J. Madera-Santana,[1] Yolanda Freile-Pelegrín,[2] José C. Encinas,[3] Carlos R. Ríos-Soberanis,[4] Patricia Quintana-Owen[2]

[1]Centro de Investigación en Alimentación y Desarrollo, A.C. Carr. a La Victoria, Km 0.6, 83304 Hermosillo, Sonora, México, Hermosillo Sonora, México

[2]Centro de Investigación y Estudios Avanzados del IPN, Unidad Mérida, Ant. Carr. a Progreso Km. 6. Apdo. Postal 73, Cordemex 97310, Mérida Yucatán, México

[3]Departamento de Investigación en Polímeros y Materiales, Universidad de Sonora, C.P. 83000 Hermosillo, Sonora, México

[4]Centro de Investigación Científica de Yucatán, A.C. Unidad de Materiales, Col. Xcumpich. Mérida, Yucatán, México

Correspondence to: T. J. Madera-Santana (E-mail: madera@ciad.mx)

ABSTRACT: Seaweed waste (SWW) is a residue or by-product from the filtration step of the agar extraction process, and it has been explored as an inexpensive and effective filler for incorporation by melt blending into a poly(lactic acid) (PLA) matrix. PLA-SWW biocomposites were manufactured with various contents of SWW (0, 5, 10, 15, and 20 wt %) using a sheet extrusion process. PLA was functionalized with maleic anhydride (MAH) by reactive extrusion using dicumyl peroxide (DCP) as an initiator, and it was extruded using 0, 5, and 20 wt %. SWW content. The mechanical, thermal, structural, and morphological properties of the processed biocomposites were investigated. Regarding the mechanical behavior, a slight increase in the tensile modulus was observed at low SWW content. The thermal properties indicated that the rigid amorphous phase content was enhanced in the biocomposites. This work suggests that SWW can be used as filler to develop environmental friendly biocomposites. © 2015 Wiley Periodicals, Inc. J. Appl. Polym. Sci. **2015**, *132*, 42320.

KEYWORDS: biodegradable; composites; extrusion; properties and characterization

Received 3 January 2015; accepted 7 April 2015

DOI: 10.1002/app.42320

INTRODUCTION

The partial replacement of petroleum-derived plastics by novel bio-based materials from inexpensive, renewable natural resources greatly impact the plastics, coatings, and composites industries, which use biodegradable matrices and bio-based byproducts as fillers.[1,2] New bio-based products from renewable resources may exhibit similar and sometimes better properties than commercial petroleum based products, and may have improved recycling and biodegradability capabilities.[3]

Among biodegradable polymeric matrices, poly(lactic acid) (PLA) is promising biodegradable aliphatic polyester resulting from the condensation polymerization of lactic acid. It has found many uses, ranging from every-day consumables to biomedical materials.[4] PLA is referred as a "green" polymer because it is available from agricultural renewable resources; hence, its production requires less fossil resources compared with petroleum-based plastics. However, the relatively high resin cost, poor impact strength, low distortion temperature, and brittleness have restricted its applicability. To overcome the existing limitations and improve the mechanical performance of PLA, some authors have studied the reinforcement of PLA with other renewable and biodegradable fillers (starch, sisal, hemp, and wood fibers).[5–8] Apart from conventional fillers, a considerable interest has been recently generated concerning the utilization of novel fillers derived from industrial waste. The conversion of such materials into fillers introduces low cost materials and a solution for the disposal of waste from various industries.

Agar is an important industrial polysaccharide that is widely used as a gelling agent in food and pharmaceutical applications. It is synthesized by marine algae and possesses unique gelling properties. It is one of the most strongly gelling hydrocolloids obtained from the cell wall of Rhodophyta (marine red seaweeds), mainly from the genera *Gelidium* and *Gracilaria*. The industry is relatively mature in terms of its manufacturing methods and market: the total volume of agar production in 2009 was 9600 tons, which was equivalent to US$173 million.[9] Chemically, agar is composed of a heterogeneous mixture of molecules, built on a

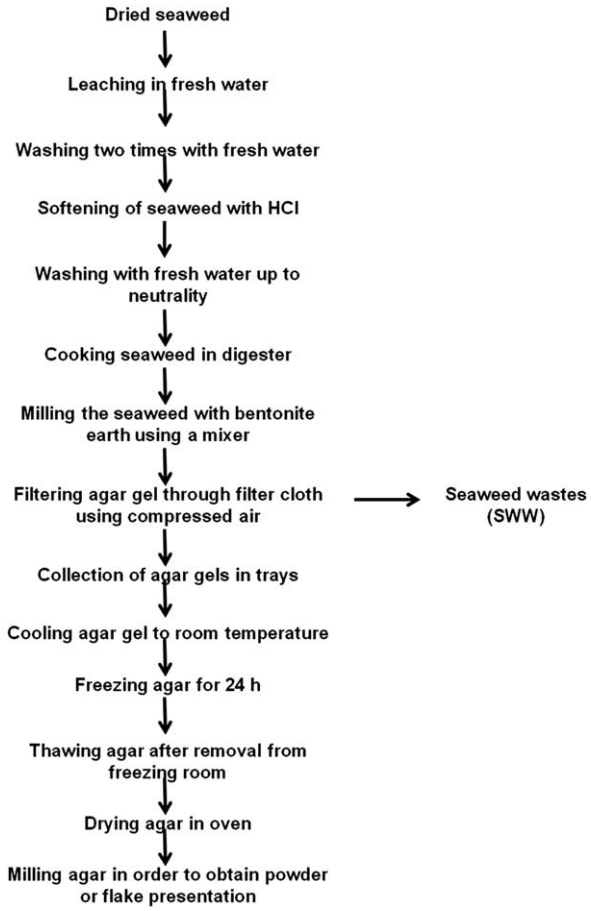

Figure 1. Scheme of agar extraction and seaweed wastes (SWW) generation.

disaccharide containing repeating units of D-galactose and 3,6-anhydro-L-galactose.[10] Substitution with sulfate, methyl ethers and/or pyruvate groups can occur at various sites in the polysaccharide chain. The conventional industrial process for agar extraction (Figure 1) includes seaweed pretreatment, extraction, filtration, concentration, and dehydration. Briefly, agar is extracted and dissolved in boiling water, often under pressure. The agar dissolved in water must be filtered to remove the residual seaweed, and the hot filtrate is cooled to form a gel containing ~1% agar. The remaining 99% is water that must be removed from the gel by a freeze-thaw process used to dewater and concentrate the gel prior to drying. A careful control of several parameters (i.e., pH, temperature, and time) is needed to obtain control of the molecular weight distribution of the polysaccharide. In the current industrial practice of producing agar, large quantities of seaweed wastes (SWW) are produced from the filtration step. A "filter cake" is generated and discarded. The "filter cake" represents ~70% of the raw material used. This "filter cake" or SWW mainly consists of the residual seaweeds enriched with cellulose and hemicellulose, as well as agar residues.[11,12] It could even contain small amounts of floridean starch.[13] The "filter cake" also contains diatomite earth, which is used as a filtration aid in the filtration step. Therefore, SWW is a material enriched with different polysaccharides that can be used as inexpensive hybrid filler in biocomposites.

Several authors have reported the use of raw seaweed biomass as a reinforcement in biocomposites with poly(butylene succinate),[1] polypropylene,[2,14,15] high density polyethylene,[16] and poly(lactic acid).[17] These biocomposites were formulated using seaweeds from the three divisions Chlorophyta, Phaeophyta, and Rhodophyta (green, brown and red algae, respectively) as a biofiller in a polymeric matrix. The results have shown that seaweeds could produce composite materials using thermoplastic matrices. These composites can be used in several applications such as in the automotive, construction or packaging industries. However, to the best of our knowledge, SWW obtained from agar extraction have not been employed as a biofiller in a polymeric matrix.

In this study, PLA-SWW biocomposites were investigated to examine the feasibility of using seaweed residues from the agar extraction process as a reinforcement material. The effect of filler addition on the structure and properties of PLA-SWW biocomposites was evaluated.

EXPERIMENTAL

Raw Materials

Poly(lactic acid) (PLA) 7001D pellets received from NatureWorks LLC (Minnetonka, MN) were used as the polymeric matrix. These pellets were milled in a Thomas Wiley® mill model 4 (Swedesboro, NJ) to facilitate feeding into the extruder. The PLA had molecular weight of 101 kDa and a density of 1.24 g/cm^3. Seaweed wastes (SWW) were obtained from the extraction of agar from *Hydropuntia cornea*[18] and described in Figure 1. The seaweed particles used had a variety of irregular shapes and sizes (262.2 ± 80.6 μm).

The mechanical properties of biocomposites depend on interfacial adhesion between the filler and polymeric matrix. To promote the filler-matrix compatibilization, maleic anhydride (MAH) and dycumyl peroxide (DCP) purchased from Sigma-Aldrich Chemical (Milwaukee, WI) were used.

Biocomposites Preparation

The compositions of the PLA-SWW biocomposites prepared in this work are listed in Table I. PLA, SWW and MAH-DCP were precisely weighed, and the content of MAH (3.5 wt %) – DCP (1.5 wt %) was fixed relative to the PLA content. Raw materials in powder form were physically mixed in a plastic bag and

Table I. Compositions of the PLA-SWW Biocomposites

Sample	PLA (wt %)	SSW (wt %)	MAH + DCP (wt %)
100/0	100	–	–
95/5	95	5	–
90/10	90	10	–
85/15	85	15	–
80/20	80	20	–
95/0/5	95	–	5
90/5/5	90	5	5
75/20/5	75	20	5

processed using a single screw mini-laboratory extruder from Polymer Evaluation Products model ATLAS (Chicago, IL), with a temperate profile of 145°C (feed zone) and 160°C (die zone). The extruder shaft (~1 cm diameter) was rotated at 60 rpm. The sheet (5 cm wide and 0.2 cm thick) was collected with a stainless steel idler roll. Finally, all sheets obtained were storage in plastic bags, before testing.

Biocomposites Characterization

Surface Color. Ribbons of PLA-SWW biocomposites obtained from the extrusion process were measured for their color values. The color was read using the Commission International de L'Eclairage (CIE) lab parameters (L^*, a^*, b^*) with a spectrocolorimeter Konica Minolta model CR-400 (Ramsey, NJ). The scanner was calibrated with a standard tile ($Y = 92.4$, $x = 0.3161$, $y = 0.3324$). In this coordinate system, the L^* value is a measure of the lightness (brightness) ranging from 0 (black) to 100 (white), the a^* value is a measure of the redness ranging from −100 (green) to +100 (red), and the b^* value is a measure of the yellowness ranging from −100 (blue) to +100 (yellow). The color differences (ΔE) were also calculated by the following equation:

$$\Delta E = \sqrt{(\Delta L^*)^2 + (\Delta a^*)^2 + (\Delta b^*)^2} \quad (1)$$

where: $\Delta L^* = L^* - L_0^*$, $\Delta a^* = a^* - a_0^*$, and $\Delta b^* = b^* - b_0^*$, L_0^*, a_0^*,and b_0^*, represent the color parameter values of the standard, and L^*, a^*, and b^* represent the color parameters of the sample. Measurements were performed by placing the film sample over the standard. All of the samples were analyzed by recording six measurements for each sample.

Thermal Properties. Differential scanning calorimetry (DSC) analysis was performed on a Perkin Elmer DSC model Pyris Diamond (Shelton, CT) under a nitrogen atmosphere. The sample temperature was increased at 50°C/min from room temperature (25°C) to 190°C, held isothermal for 4 min order to eliminate any previous thermal history, and cooled down to 25°C at 10°C/min. The sample was reheated to 190°C at 10°C/min, held isothermal for 2 min, and cooled down to 25°C at 10°C/min, to trace the thermal behavior. From the thermograms of the individual PLA-SWW biocomposites, the glass transition temperature (T_g), specific heat change (ΔC_p), enthalpies of melting (ΔH_m) and crystallization just before melting (ΔH_c), and temperatures of crystallization (T_c), and melting (T_m) were determined. The fractions of the existing possible PLA phases, the crystalline (X_c), the mobile amorphous (X_{ma}) and the rigid amorphous (X_{ra}) phases, were calculated using a three-phase model reported by Zuza *et al.*[19]

$$\chi_c(\%) = \frac{\Delta H_m - \Delta H_c}{\Delta H_m^\circ} \times \frac{100}{w} \quad (2)$$

$$\chi_{ma}(\%) = \frac{\Delta C_p}{\Delta C_p^\circ} \times 100 \quad (3)$$

$$\chi_{ra}(\%) = 100 - \chi_c - \chi_{ma} \quad (4)$$

where w is the PLA weight fraction in the blend and, ΔH_m and ΔH_c are the experimental enthalpies of melting and crystallization just before melting, respectively. ΔH°_m is the enthalpy of melting for 100% crystalline PLA (93.6 J/g), ΔC_p is the specific heat change at T_g and ΔC°_p is the specific heat change at T_g of fully amorphous PLA (0.628 J $g^{-1}°K^{-1}$).[19] Thermal decomposition analyses were performed using a thermogravimetric analyzer (TGA, Perkin Elmer model TGA-7, Waltham, MA). Approximately 10 mg of sample were heated from 50 to 600°C at 10°C/min under a nitrogen atmosphere with a flow rate of 60 mL/min.

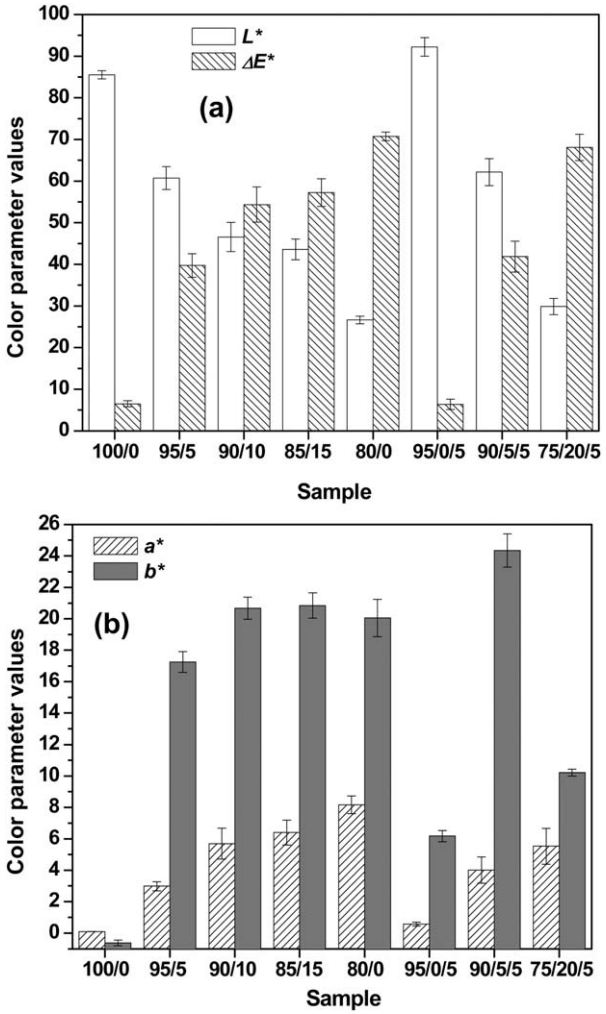

Figure 2. Color parameters of PLA-SWW biocomposites: (a) L^* and ΔE, and (b) a^* and b^*.

Mechanical Properties. A dumbbell-shape geometry according to ASTM D1708-02 was used for tensile testing of the samples. This test was performed using a universal testing machine (United model SSTM-5kN, Huntington Beach, CA) at a crosshead speed of 10 mm/min. The tensile strength, elongation at break, and tensile modulus were determined, and at least six specimens of each formulation were tested.

Structural Analysis. Infrared spectra in the attenuated total reflection mode (ATR-FTIR) were obtained at room temperature using a Thermo Nicolet spectrometer model Nexus 670-FTIR (Madison, WI). The PLA-SWW biocomposites were analyzed in the 4000−600 cm^{-1} range with 4 cm^{-1} resolution. To determine the crystalline structure of the extruded PLA-SWW biocomposites, a sample of 1 × 1 cm^2 was placed in a sample

Table II. Thermal Properties of the PLA-SWW Biocomposites Determined by DSC

Sample	T_g (°C)	ΔC_p (J/g°C)	T_c (°C)	ΔH_c (J/g)	T_m (°C)	ΔH_m (J/g)	χ_c (%)	χ_{ra} (%)	χ_{ma} (%)
100/0	58	0.57	105.6	28.4	144.7	31.4	3.2	6.0	90.8
95/5	57.3	0.51	98.8	27.6	151.3	32.3	5.3	13.4	81.3
90/10	56.8	0.41	95.2	21.9	151.3	24.8	3.4	31.2	65.4
85/15	56.6	0.37	96	22.7	152.1	23.8	1.4	39.7	58.9
80/20	56.8	0.13	93.6	22.6	150.9	23.1	0.7	78.6	20.7
95/0/5	57.8	0.48	102.3	27.7	151.8	31.5	4.0	19.6	76.4
90/5/5	57.5	0.37	79.1	23.9	151.5	29.4	6.5	33.5	60.0
75/20/5	57.2	0.28	89.5	21.8	150.9	22.7	1.2	53.9	44.9

holder for X-ray diffractometry. The X-ray diffraction patterns were recorded in reflection mode in, an angular range of 5−60° (2θ), and at room temperature using a diffractometer (Siemens model D5000, GK Germany), which operated at a CuKα wavelength of 1.542 Å. The radiation from the anode operating at 34 kV and 20 mA was used for tests.

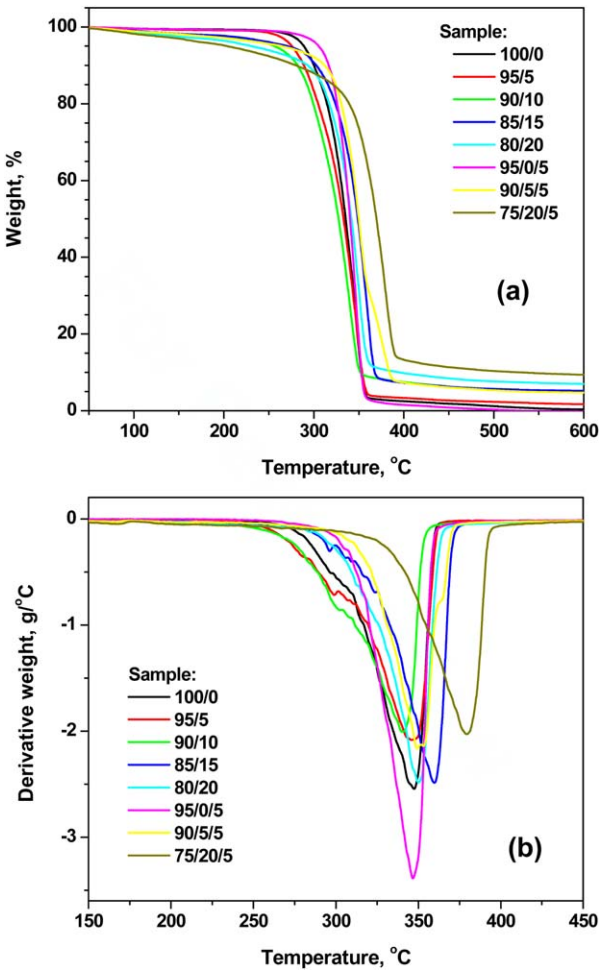

Figure 3. TGA thermograms of PLA-SWW biocomposites: (a) TGA, and (b) DTGA. [Color figure can be viewed in the online issue, which is available at wileyonlinelibrary.com.]

Interfacial Morphological Analysis. Morphological studies of cryogenically fractured samples of PLA-SWW biocomposites were performed using a scanning electron microscope (SEM), from FEI Corp. model Philips XL30 ESEM-FEG (Hillsboro, OR). The samples were coated with a thin layer of Au-Pd using a sputter coater (Quorum model QI5OR-ES, Sussex, UK) prior to scanning. The morphological analysis of the PLA-SWW biocomposites was performed to investigate the SWW dispersion and interfacial adhesion of the filler in the PLA matrix.

Statistical Analysis. The experimental data obtained were statistically analyzed by one-way analysis of variance (ANOVA) using NCSS 2007 (NCSS LLC. Kaysville, UT). The significance of each mean of property was determined ($P < 0.05$) to evaluate the effect of the SWW content and compatibilization on the thermal, optical and mechanical properties of the biocomposites.

RESULTS AND DISCUSSION

Apparent Color of the Biocomposites

Color is an important attribute of commercial composites and biocomposites. In this study, the extruded PLA-SWW biocomposites were uniform and rigid with rough surfaces. The color changes were the result of the SWW content variation in the PLA matrix. Figure 2 shows the CIE lab parameters for all of the compositions. In Figure 2(a) the luminosity values (L^*) showed a gradual decrease as the SWW content increased. The compatibilization treatment with MAH-DCP in samples 95/0/5, 90/5/5, and 75/20/5 showed changes in the L^* values in comparison with neat PLA, where a significant decrease ($P < 0.05$) was observed at higher SWW content. The reduction of the L^* values could be

Table III. TGA Characterization of the PLA-SWW Biocomposites

Sample	T_5 (°C)	T_{25} (°C)	T_{50} (°C)	T_{75} (°C)	T_{dp} (°C)
100/0	290.2	319.6	335.5	346.1	346.4
95/5	276.1	310.9	332.9	346.0	346.3
90/10	255.8	304.9	327.2	341.0	339.6
85/15	266.1	330.1	348.8	359.7	359.3
80/20	235.5	323.1	341.6	352.1	350.1
95/0/5	307.3	328.8	340.1	348.1	346.3
90/5/5	272.3	334.9	350.1	368.7	351.3
75/20/5	208.6	348.0	369.1	382.5	378.9

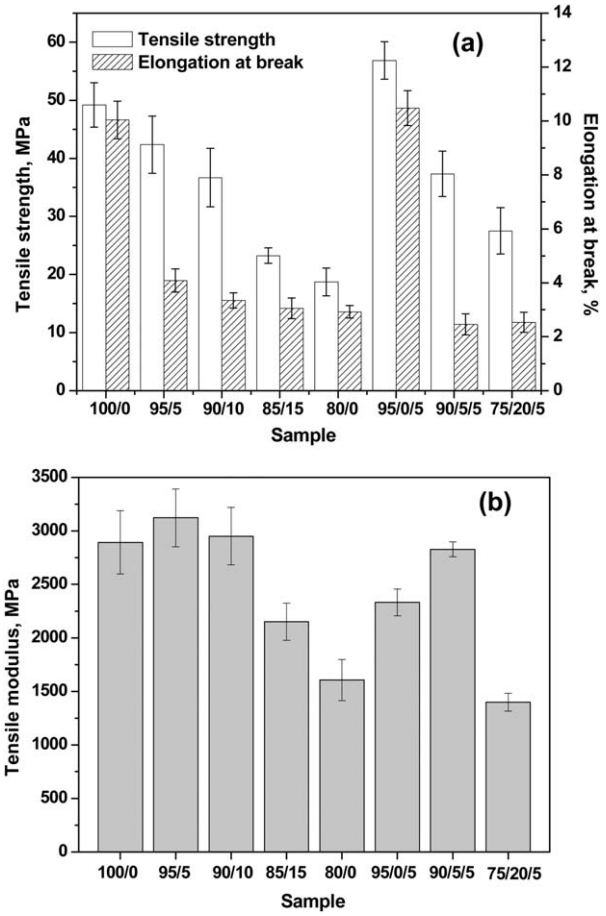

Figure 4. Mechanical properties of PLA-SWW biocomposites: (a) tensile strength and elongation at break, and (b) tensile modulus.

attributed to a close vicinity of the SWW filler in the PLA matrix that produces low brightness in the biocomposites. However, the opposite behavior was observed in the color difference (ΔE). This result was somewhat expected because ΔE is closely related to the SWW content, and this parameter shows the combined effects of the three color parameters (L, a, and b). The addition of SWW and MAH-DCP to the PLA matrix significantly modified ($P < 0.05$) the ΔE value obtained from the biocomposites. In the same sense, the color parameters a^* (red−green) and b^* (yellow−blue) showed a gradual increase in their values Figure 2(b), although the b^* parameter reached a constant value when the SWW content was 10 wt %. The addition of MAH-DCP in sample 90/5/5 produced a significant increase ($P < 0.05$) in this parameter, in comparison with all of the other formulations. Nevertheless, the increase of the SWW content (sample 75/20/5) showed a significant decrease ($P < 0.05$) in this parameter compared with sample 80/20, which had the same SWW content but without compatibilization. Moreover, the decrease in the L^* values with an increase in the b^* values indicated that a yellowish tint appeared in the biocomposites. This result was in agreement with the visible observation.

Thermal Properties

The thermal properties of the neat PLA and PLA-SWW biocomposites are listed in Table II. The DSC thermograms (data not shown) of each biocomposite exhibit clear specific heat changes such as the glass transition, an exothermal crystallization peak, and an endothermic melting peak during heating. The T_g values of the PLA-SWW biocomposites were slightly affected by the presence of SWW, because a slight decrease from 58°C to 56.6°C was observed. The T_g values of the PLA-SWW biocomposites with compatibilization treatment remained unchanged, likely due to the improvement in the interfacial interaction between the SWW and PLA. The PLA-SWW biocomposites with and without compatibilization treatment were affected in their crystallization behavior and showed lower crystallization temperature (T_c) and enthalpy (ΔH_c) in comparison with neat PLA. Moreover, neat PLA showed a narrow melting peak at 144.7°C, whereas the PLA-SWW biocomposites displayed a slightly higher melting temperature (150.9−152.1°C). The increase in T_m could be attributed to the presence of the SWW filler in the PLA matrix. The enthalpy of melting (ΔH_m) is an important parameter for crystallization and the biocomposites showed a decrease in their ΔH_m values compared with neat PLA (an exception was seen in sample 95/5). This decrease signifies the negative influence on crystallinity due to the interaction between the SWW filler and the PLA matrix. In addition, the SWW filler restricts the mobility of the PLA chains. A similar behavior was reported by Luan *et al.*[2] in seaweed fibers and PP composites. The calculated crystallinity (X_c) for the neat PLA and PLA-SWW biocomposites ranged from 0.7 to 6.5%. The increase in X_c observed in samples 95/5 and 90/5/5 could suggest that at these formulations, the SWW served as nucleating sites for crystallization and enhanced the rate of crystallization. The X_c of samples 100/0 and 95/0/5 was 3.2 and 4%, respectively. However, the increase of the SWW content reduced the X_c of PLA-SWW biocomposites. Similar, X_c values have been reported in PLA-wood composites.[20] Moreover, the rigid amorphous phase (X_{ra}) in the PLA-SWW biocomposites increased from 13.4 to 78.6% compared with the neat PLA (6%). In contrast, the mobile amorphous phase (X_{ma}) decreased from 90.8% (neat PLA) to 20.7 and 44.9% in samples 80/20 and 75/20/5, respectively. This result could indicate that the

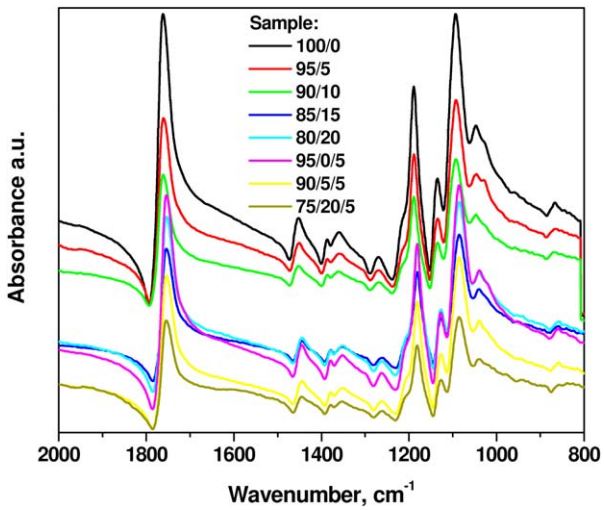

Figure 5. FTIR spectra of PLA-SWW biocomposites. [Color figure can be viewed in the online issue, which is available at wileyonlinelibrary.com.]

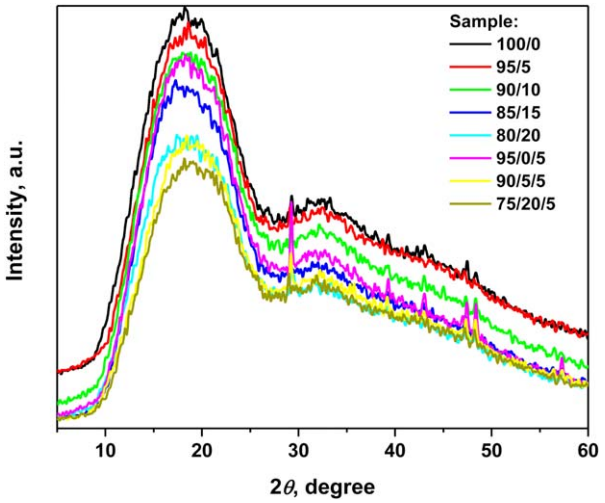

Figure 6. XRD patterns of PLA-SWW biocomposites. [Color figure can be viewed in the online issue, which is available at wileyonlinelibrary.com.]

SWW content affects the development of rigid amorphous phases in PLA-SWW biocomposites.

The thermogravimetric analysis (TGA) [Figure 3(a)], and DTGA [Figure 3(b)] thermograms under a nitrogen atmosphere was applied to measure the thermal stability of the neat PLA and PLA-SWW biocomposites. In general, there was one degradation stage throughout the temperature runs [Figure 3(a)]. Nevertheless, the DTGA thermograms showed small shoulders associated with degradation of the components from the biocomposites. The neat PLA had a decomposition temperature (T_{dp}) at 346°C; however, the incorporation of 20 wt %. SWW shifted this temperature to 350 and 379°C in samples 80/20 and 75/20/5, respectively. Moreover, the thermal stability of the biocomposites filled with compatibilizer showed a significant improves compared with the untreated ones. The thermal decomposition temperatures with 5, 25, 50, and 75% weight loss (T_5, T_{25}, T_{50}, and T_{75}, respectively) are listed in Table III. At 300°C, there were weight losses ranging from 9.5 to 21% and 3.7 to 12% for the untreated and treated PLA-SWW biocomposites, respectively. The improvement in the thermal stability of the biocomposites with compatibilization treatment could indicate that the compatibility and interfacial bonding increased. Similar results have been reported by Huda *et al.*[7] for wood-fiber-reinforced PLA composites.

Mechanical Properties

The tensile properties of the PLA-SWW biocomposites are shown in Figure 4(a,b). The tensile strength and elongation at break decreased with the addition of SWW. A decrease in tensile strength with 5 and 10 wt % SWW content was observed; however, at 15 and 20 wt % of SWW content, this parameter is much lower than the PLA control. The compatibilization treatment performed to the biocomposites significantly increased ($p < 0.05$) the tensile strength, mainly in the formulation with 20 wt % SWW. This result indicates good adhesion between the SWW filler and PLA matrix. In contrast, the elongation at break of the untreated and treated biocomposites showed a drastic decrease reaching a minimum value (2.8%) when the SWW content was 20 wt %. The decrease in the elongation at break is due to the increased stiffness of the biocomposites when the SWW content was increased, and this is a common characteristic of reinforced thermoplastic composites. Furthermore, the low elongation of the SWW filler restricts the flow of polymer molecules past one another.[21] The average tensile modulus increased with the addition of 5 and 10 wt % SWW content, however, further addition of SWW filler decreased the modulus. At 20 wt % of SWW filler, this property was 42% and 49% lower in comparison with neat PLA for biocomposites with and without compatibilization treatment, respectively. Several studies in which neat PLA and organic fillers were mixed without coupling agents have been conducted to produce biocomposites,[22,23] although these studies show a marked reduction in the tensile strength and elongation at break and an increase in the tensile modulus as the filler concentration increases. From our results, the use of compatibilization (i.e., maleation) improves the mechanical properties of the resultant composites. Similar results were observed in biocomposites of PLA with cottonseed burs and hulls.[23]

Structural Analysis

The FTIR spectra of the PLA-SWW biocomposites in the range of 2000−800 cm^{-1} are shown in Figure 5. The spectra of PLA-SWW and PLA are similar, and it appears that the SWW filler were encapsulated inside the PLA matrix. However, the FTIR-spectra are useful to elucidate the existence and type of interaction that might occur between the molecules of PLA and SWW. Figure 5 clearly shows that the neat PLA and PLA-SWW biocomposite show six peaks (1745, 1445, 1350, 1265, 1183, and 1085 cm^{-1}). The band at 1755 cm^{-1} represents the C═O stretch and the O─C═O stretch at 1183 cm^{-1}, and both peaks are characteristic of ester bonds.[24] The bonds at 1445 and 1350 cm^{-1} are attributed to bending deformation of the CH_3 groups. The peaks situated at 1265 and 1085 cm^{-1} are related to the anhydrides (C─CO─O─CO─C) valence vibration, as well as to the 3,6-anhydro-galactose bridge of agar.[25] As observed in Figure 5, the addition of SWW produced a reduction in the spectra intensity, even in the samples with compatibilization treatment. The band originating from the C═O stretching vibration was situated at 1745 cm^{-1} for neat PLA and, showed alternations as the SWW content increased and when chemical modification was performed in the biocomposite. The amount of MAH present in the biocomposites (samples 95/0/5, 90/5/5, and 72/20/5) is small; the stretching of MAH is very weak and might overlap with the carbonyl group of PLA. Perhaps, the extent of grafting is too low and the FTIR could not be sensitive enough to identify the changes. A similar feature has been reported by Orozco *et al.*[24]

The effect of the SWW filler on the crystallization behavior of the PLA was studied using X-ray diffraction as shown in Figure 6. The diffraction pattern of PLA shows one broad peak with a maximum at $2\theta = 18.8°$ and a small peak at $2\theta = 29.45°$. The pattern of the former peak remained unaffected upon addition of SWW filler. This result is fairly similar to results found in the literature,[26,27] in which the diffraction peak is centered at 2θ between 16.4° and 25.3°. The diffraction peaks observed in

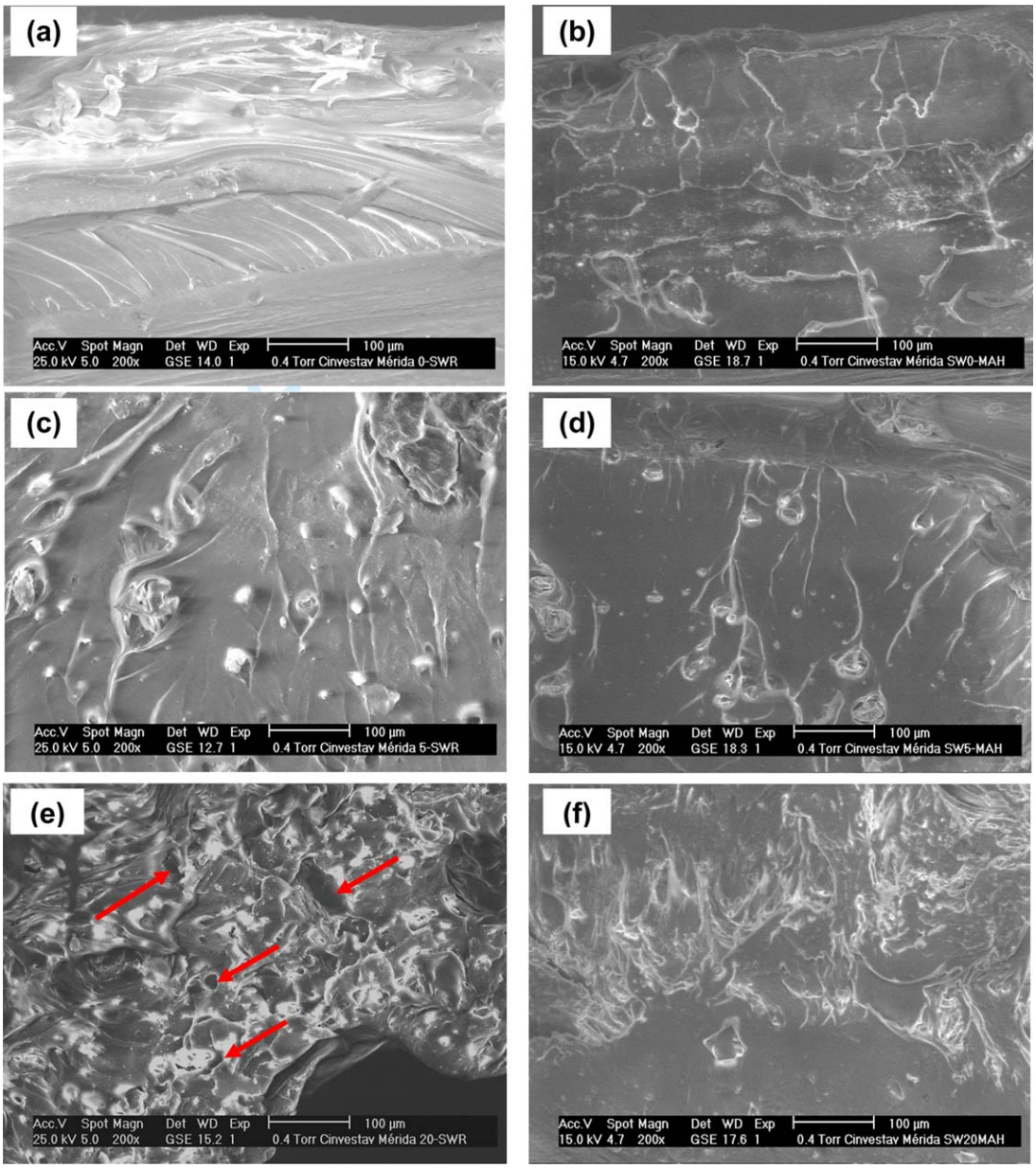

Figure 7. SEM micrographs showing cryogenically fractured surface of PLA-SWW biocomposites: (a) 100/0, (b) 95/0/5, (c) 95/5, (d) 90/5/5, (e) 80, and (f) 75/20/5. [Color figure can be viewed in the online issue, which is available at wileyonlinelibrary.com.]

Figure 6 originated from the former diffraction peak, which corresponds to α form PLA crystals centered at $2\theta = 18.8°$, and the gradual reduction in the intensity among the samples was due to the difference in the relative crystallinity. In contrast, the peaks situated at 29.4°, 47.4°, and 48.4° could be attribute to the diatomite earth (which contains calcite) used during the agar extraction process, and the clay used to hold the sample during analysis.

Surface Morphology

The interfacial morphology of the PLA-SWW biocomposites was examined using SEM characterization in Figure 7, and the micrograph number indicates the sample code. The micrographs at 200× magnification were compared and analyzed as a function of the SWW content (between rows) and the compatibilization treatment (between columns). The PLA matrix is shown in Figures 7(a,b), a homogenous and smooth surface structure can be observed. However, the addition of SWW produces an increase of porosity on the biocomposite surfaces. The morphologies observed in Figures 7(c,d) did not show significant microstructural differences. In contrast, Figure 7(e), which had the highest SWW content and no treatment, showed the presence of voids and defects (indicated by the arrows). This result could be attributed to poor dispersion and adhesion at the SWW and PLA matrix interface. The formation of SWW agglomerates in this formulation contributes to the decrease in the mechanical properties of the biocomposites, as observed in Figure 4. Finally, Figure 7(f) shows that the compatibilization

treatment improved the dispersion and the adhesion of SWW in the PLA matrix.

CONCLUSIONS

To the best of our knowledge, this study could be the first report of the manufacture of biocomposites using seaweed wastes (SWW) from an agar extraction process and PLA as a matrix. The color parameter values of the samples indicated that an increase in the SWW content caused a yellowish tint in the biocomposites, it is due to good dispersion of SWW into PLA matrix. PLA matrix with low SWW content showed the highest crystalline phase (X_c), because SWW act as nucleating sites. The increase of the rigid amorphous phase (X_{ra}) in the PLA-SWW biocomposites, mainly with compatibilization treatment, was associated with improved thermal stability. The increase of the SWW content reduced the tensile strength and elongation at break of the PLA-SWW biocomposites, but increased the stiffness at low SWW contents, it is a common characteristic of reinforced thermoplastic. The compatibilization treatment only improves the tensile strength of the PLA and biocomposites. The formulated biocomposites have shown particular interactions due to the SWW filler was encapsulated inside the PLA matrix and the possible formation of secondary bonds, as was analyzed using FTIR and XRD. SEM characterization showed that the compatibilization treatment improved the interfacial adhesion between the SWW and PLA.

Overall, the advantage of using a biodegradable polymer such as PLA as a matrix and SWW as filler has demonstrated that this biocomposite has good thermal and mechanical properties. Furthermore, the use of SWW as filler in PLA provides an interesting alternative for the production of low-cost and ecologically friendly biocomposites.

ACKNOWLEDGMENTS

The authors are grateful to Mrs. C. Chavez, A. Cristobal, Mr. D. Aguilar Treviño of CINVESTAV IPN Unidad Merida, and Mr. J. Laviada of CICY Unidad de Materiales for their technical assistance. Part of this research was conducted in facilities of LANNBIO at CINVESTAV-Mérida under the projects FOMIX-Yucatán 2008–108160 and CONACYT LAB-2009-01 No. 123913.

REFERENCES

1. Lee, M. O.; Han, S. O.; Seo, Y. B. *Comp. Sci. Technol.* **2008**, *68*, 1266.
2. Luan, L.; Wu, W.; Wagner, M. H.; Mueller, M. *J. Appl. Polym. Sci.* **2010**, *118*, 997.
3. Mohanty, A. K.; Misra, M.; Drzal, L. T. *J. Polym. Environ.* **2002**, *10*, 19.
4. Auras, R.; Lim, L. T.; Selke, S. E.; Tsuj, H. In Poly (lactic acid): Synthesis, Structure, Properties, Processing and Applications. Wiley: Hoboken, NJ, **2010**.
5. Martin, O.; Schwach, E.; Averous, L.; Couturier, Y. *Starch* **2001**, *53*, 372.
6. Petersson, L.; Kvien, I.; Oksman, K. *Compos. Sci. Technol.* **2007**, *67*, 2535.
7. Huda, M. S.; Drzal, L. T.; Misra, M.; Mohanty, A. K. *J. Appl. Polym. Sci.* **2006**, *102*, 4856.
8. Wang, Y.; Tong, B.; Hou, S.; Li, M.; Shen, C. *Compos. Part A Appl.* **2011**, *42*, 66.
9. Bixtler, H. L.; Porse, H. *J. Appl. Phycol.* **2011**, *23*, 321.
10. Armisén, R.; Galatas, F. In Handbook of Hydrocolloids, 2nd ed.; Phillips, G. O.; Williams, P. A., Eds. Woodhead Publishing: UK, **2009**.
11. Baldan, B.; Andolfo, P.; Navazio, L.; Tolomio, C.; Mariani, P. *Eur. J. Histochem.* **2001**, *45*, 51.
12. Kraan, S. In Carbohydrates-Comprehensive Studies on Glycobiology. InTech, **2012**.
13. Freile-Pelegrín, Y.; Murano, E. *Biores. Technol.* **2005**, *96*, 295.
14. Masudul Hassan, M.; Mueller, M.; Wagners, M. H. *J. Appl. Polym. Sci.* **2008**, *109*, 1242.
15. Jang, Y. H.; Han, S. O.; Sim, I. N.; Kim, H.-II. *Compos. Part A Appl.* **2013**, *47*, 83.
16. Albano, C.; Karan, A.; Dominguez, N.; Sanchez, Y.; González, J.; Aguirre, O.; Cataño, L. *Compos. Struct.* **2005**, *71*, 282.
17. Sim, K. J.; Han, S. O. *Macromol. Res.* **2010**, *18*, 489.
18. Freile-Pelegrín, Y.; Robledo, D. *J. Appl. Phycol.* **1997**, *9*, 533.
19. Zuza, E.; Ugartemendia, J. M.; Lopez, A.; Meaurio, E.; Lejardi, A.; Sarusua, J. R. *Polymer* **2008**, *49*, 4427.
20. Gregorova, A.; Hrabalove, M.; Kovalcik, R.; Wimmer, R. *Polym. Eng. Sci.* **2011**, *51*, 143.
21. Ayrilmis, N.; Kaymakci, A.; Ozdemir, F. *J. Ind. Eng. Chem.* **2013**, *19*, 908.
22. Finkenstadt,V. L.; Tisserat, B. *Ind. Crops Prod.* **2010**, *3*, 316.
23. Sutivisedsak, N.; Cheng, N. H.; Dowd, M. K.; Selling, G. W.; Biswas, A. *Ind. Crops Prod.* **2012**, *36*, 127.
24. Orozco, V. H.; Brostow, W.; Chonkaew, W.; Lopez, B. J. *Macromol. Symp.* **2009**, *277*, 69.
25. Freile-Pelegrín, Y.; Madera-Santana, T.; Robledo, D.; Veleva, L.; Quintana, P.; Azamar, J. A. *Polym. Deg. Stabil.* **2007**, *92*, 244.
26. Kuwabara, K.; Gan, Z.; Nakamura, T.; Abe, H.; Doi, Y. *Biomacromol.* **2002**, *3*, 390.
27. Yeh, J. T.; Tsou, C. H.; Huang, C. Y.; Chen, K. N.; Wu, C. S.; Chai, W. L. *J. Appl. Polym. Sci.* **2010**, *116*, 680.